ELEVENTH EUROPEAN ROTORCRAFT FORUM

Paper No. 63

AN APPLICATION OF FLOQUET THEORY TO INVESTIGATE HELICOPTER MECHANICAL INSTABILITY USING A SPATIAL MODEL INCLUDING ROTOR BLADE FLAPPING

Jochen Ewald

Institute of Flight Mechanics
Technische Universität Braunschweig

September 10-13, 1985
London, England.

THE CITY UNIVERSITY, LONDON, EC1V OHB, ENGLAND.

AN APPLICATION OF FLOQUET THEORY TO INVESTIGATE HELICOPTER MECHANICAL INSTABILITY USING A SPATIAL MODEL INCLUDING ROTOR BLADE FLAPPING

J. Ewald
Institute of Flight Mechanics
Technische Universität Braunschweig

1. Abstract

The classical method developed by Coleman and Feingold to investigate ground resonance uses a planar model only including the lead-lag motions of rotor blades. Comprehensive investigations study the ground resonance with a spatial model with the result, that there exist more possible regions of mechanical instability.
This paper presents a spatial helicopter model including blade flapping and consequently the coupling effects of rotor blade lag-flap motion. Floquet theory is used to solve the linearized equations of motion with periodically varying coefficients to investigate the influence of different blade characteristics such as different damping, mass and stiffness distribution.

2. Notation

$\underline{\underline{A}}$	-	matrix of first order system
a_o, a_1, b_1, b_o	-	flap-coefficients
a	-	distance flap hinge to hub
$\underline{b}_k$	-	eigenfunction of the system with periodically varying parameters
$c_{a\alpha}$, c_{WO}, c_{W2}	-	profile parameters
c_ζ, c_β	-	stiffness parameters of rotor blade
c_x, c_y, c_ϕ, c_θ	-	stiffness parameters of fuselage
$\underline{\underline{C}}$	-	stiffness matrix
$\underline{\underline{D}}$	-	damping matrix
d_x, d_y, d_ϕ, d_θ	-	damping parameters of fuselage
d_ζ, d_β	-	damping parameters of rotor blade
e_o, e_1, f_1, f_o	-	lag-coefficients
e	-	distance flap hinge to lag hinge
g	-	acceleration due to gravity
I_{xx}	-	moment of inertia (roll)
I_{yy}	-	moment of inertia (pitch)
$\underline{\underline{M}}$	-	matrix of masses and moments of inertia
m	-	mass of fuselage
m_b	-	mass of one blade
R	-	radius of rotor disc
$\underline{r}$	-	vector from centre of gravity of the helicopter to one point of the blade
T	-	period of the periodic coefficients
V_n	-	velocity normal to the blade
V_t	-	velocity tangential to the blade
$\underline{x}$	-	vector of coordinates (second order system)
$\underline{y}$	-	vector of coordinates (first order system)
x, y,	-	degrees of freedom of the fuselage
x_s, y_s, z_s	-	position of the centre of the hub in the body-fixed coordinate system
$(e^{\lambda t})$	-	vector of eigenvalues
β, ζ	-	degrees of freedom of the rotor blade
ϑ_o, ϑ_c, ϑ_s	-	collective and cyclic pitch
$\Delta(...)$	-	perturbation value
δ_k	-	real part of λ_k
ω_k	-	imaginary part of λ_k
ω_k^*	-	frequency obtained by Floquet-theory
λ_k	-	eigenvalue of the corresponding system matrix with constant coefficients.
Λ_k	-	eigenvalue of Monodromy matrix
Ω	-	rotor speed
$\underline{\underline{\Phi}}(t)$	-	transition matrix
$\underline{\underline{\Phi}}(t=T)$	-	Monodromy matrix
ρ	-	density of air

3. Introduction

The phenomenon of mechanical instability of helicopters on the ground known as ground resonance arises due to self-exited vibrations. This is caused by blade movement in the rotor plane which leads to a change in the rotor centre of gravity away from the rotor axis. The energy for the self-excited vibrations is extracted from the rotor energy in the process. Basic investigations into ground resonance have been carried out by A. M. Feingold and R. P. Coleman [1]. They used a two-dimensional substitute model in which the air-frame is represented by two different masses m_x, m_y in the helicopter-fixed coordinate system. The landing gear is represented in ideal circumstances by springs c_x, c_y and dampers d_x, d_y. The blade properties are characterised by the point mass m_b, its radial position and the distance of the lag-hinge to the rotor hub. This planar model is useful to obtain an explanation of the phenomenon of ground resonance. However as the work of R. Schröder [2] shows, this model does not permit a complete reduction of size in the real helicopter. The position of the prevailing momentum pole is important for the movement of the three-dimensional helicopter which is composed of translations and rotations. Neglecting the motion in the z-direction (translation and yaw) likewise the lead-lag motion of the rotor blades, the rigid helicopter has 4 degrees of freedom. It can be shown that only two of the describing differential equations are coupled. Two equations give the longitudinal movement and two give the latitudinal movement. Two positions exist as momentum poles for each movement - one upper and one lower. Therefore two two-dimensional systems must be applied to reduce the three-dimensional model where at each time the lower or upper pole positions of the uncoupled longitudinal and latitudinal movement are combined respectively. Only a helicopter with properties identical in x- and y-directions can be completely reduced by two two-dimensional models. On the other hand if the airframe has asymmetrical system parameters an excitation with an eigenfrequency of the spatial system leads of course to a vibration of the planar system having the same eigenfrequency. In the direction vertical to this movement, however, there is a forced vibration which can differ from the amplitude in the three-dimensional system. If the lead-lag motion of the rotor blades is included in the reduction of the three-dimensional system, then the longitudinal and lateral movements are coupled by the rotor. The positions of the momentum poles from which the parameters of the two-dimensional model are calculated are now functions of the rotor revolution speed.

Another problem arises with the different numbers of degrees of freedom and thus, of the natural vibrations between the three-dimensional helicopter and the descriptive two-dimensional models. It is therefore of more use to conduct investigations into ground resonance using three-dimensional substitute helicopter models right from the outset. This necessitates the inclusion of aerodynamic damping and thus also of the flapping movement of the rotor blades in the investigation. And therefore a three-dimensional helicopter model is used for the following investigation into ground resonance. The theory of Floquet-Liapunow is employed for stability investigations. In addition, the problem of determining the frequency of vibrations and possible solutions are considered.

4. Equations of Motion

Similary, as in the work of M. N. Nahas [3], a three-dimensional helicopter model forms the basis of ground resonance investigations in which the following degrees of freedom should be taken into consideration

Translation in x-direction
Translation in y-direction
Roll and pitch .

In ideal circumstances the landing gear is characterised by springs and dampers with linear properties. Fig 2 shows the relation of the airframe to its surroundings. The blade is assumed as being rigid. It is connected to the rotor head by means of a drag and flapping hinge. To include rotor blades with elastic connections in the investigation a spring is inserted into each hinge which replaces the basic flexing vibration of the rotating blade with an equivalent flap or lag motion. The structural damping is taken into consideration by means of a damper in every hinge. Fig. 3 shows the replacement blade system. The grouping of the hinges as shown in Fig. 3 represents an elastic blade being rather more rigid in the lag than the flap direction. The investigation should be carried out for a 4-blade rotor so that 8 degrees of freedom are added to the four degrees of freedom of the airframe. The blade torsion is not to be considered.

In order to calculate the mass forces the absolute acceleration must be determined which is composed of the directional acceleration of the helicopter, the relative acceleration of the blade opposite the airframe as well as the coriolis and centrifugal acceleration at every point of the blade. The entire acceleration of a point on a flapping and lagging blade is shown in the appendix.
The mass force resulting amounts to: $\underline{F}_\mu = \int - \ddot{\underline{r}}\, dm$.

Considering the weight as well, the term $\underline{F}_G = \int \underline{g}\, dm$

is still to be added in which g is the earth acceleration vector in the body-fixed coordinate system. The following formulation is made for the air drag

Normal force: $dF = c_a\, \rho/2\, V_t^2\, l\, dr$

Tangential force: $dT = c_t\, \rho/2\, V_{res}^2\, l\, dr$

Only the linear range of the lift is considered so that the following simple relation can be established $c_a = c_{a\alpha}\, \alpha_{eff}$.

In order to be able to examine the influence of the cyclic control which induces the flapping motion the following formulation for the blade pitch angle is introduced:

$$\vartheta = \vartheta_o + \vartheta_c \cos\psi + \vartheta_s \sin\psi \quad .$$

The normal force and tangential force components of air drag result in

$$dF = c_{a\alpha}\, \rho/2\, (V_N\, V_T + \vartheta V_T^2)\, l\, dr$$

$$dT = \rho/2\, l\, [- c_{a\alpha}\, (V_N^2 + \vartheta V_N\, V_T) + c_{Wo} + c_{W2}\, (V_N + \vartheta V_T)^2]dr \quad .$$

The speed components V_T orthogonal to the longitudinal blade axis in the rotor plane and V_n normal to the blade tip plane are caused by derivation of the vector of any blade point: (Equation (3) and (4) in the appendix). The induced inflow is assumed to be constant above the rotor rotary disk and is calculated according to blade element theory as:

$$w_i = \Omega R \left(- \frac{D_2\, c_{a\alpha}\, l_o}{2\pi\, R} + \sqrt{\left(\frac{D_2\, c_{a\alpha}\, l_o}{2\pi\, R}\right)^2 + \vartheta_o\, D_3\, \frac{c_{a\alpha}\, l_o}{\pi\, R}} \right)$$

With the help of these terms all the forces affecting the rotor blades can be calculated.

The equations of motion thus result from the balance of forces and moments in the four degrees of freedom of the entire helicopter as well as from the balance of moments of each blade around the lag and flap hinge. The coupling of the flapping and lagging motion dues to air and mass forces, in particular to the coriolis force. The blade pitch hinge is to be situated outside the drag and flap hinge. Moreover, the control of the blade is to be free of interference with the flapping or lagging motion. If these conditions are not assumed, i. e. the pitch hinge is located inside of the lag and flap hinge, the coupling of pitch flapping, pitch lagging as well as an additional structural coupling as described by D. P. Schrage and D. A. Peters [4] are to be considered. These influences are disregarded here.
A problem in the inclusion of the coriolis forces is the non-linearity of the blade coordinates contained in them as well as in their differentiations. For example, the coriolis force resulting from the rotation of the rotor and flapping motion which has an effect on the lagging motion is valid for $dF_{co} = dm\, 2\, \Omega\, (e + b)\, \dot{\beta}\, \sin\beta$, where $\sin\beta \approx \beta$

can be assumed. This expression can not be applied in a linearization of the equations of motion although the influence on the lagging motion is greater than that of the air drag (see Just [3]). In order to overcome these problems W. Just [5] and G. Reichert [6] introduced a quasi stationary formulation for the flapping motion:

$$\beta = a_o - a_1 \cos\psi - b_1 \sin\psi$$

In doing so the flapping motion was not strictly be interpreted as the degree of freedom of the blade. However, perturbationvalues can be inserted for the coefficients so that the coefficients also named multiblade coordinates ([7] and [8]) consist of a constant part and a small temporal irregularity. For the angle of flapping β_k (t) of the k-th blade one obtains:

$$\beta_k(t) = a_o + \Delta a_o(t) - (a_1 + \Delta a_1(t)) \cos\psi_k(t) - (b_1 + \Delta b_1(t)) \sin\psi_k(t) - \Delta b_o(t) \ (-1)^{k-1}$$

and accordingly for the angle of lagging:

$$\varphi_k(t) = e_o + \Delta e_o(t) + (e_1 + \Delta e_1(t)) \cos\psi_k(t) + (f_1 + \Delta f_1(t)) \sin\psi_k(t) + \Delta f_o(t) \ (-1)^{k-1} .$$

The coefficients b_o and f_o and thus the differential form of the multiblade coordinates have to be considered as the investigation of a 4-blade rotor should be carried out. The formulations for arbitrary n-bladed rotors are to be found in detail in the work of W. Johnson [7], K. H. Hohenemser and S. K. Yin [8] as well as J. Dugundji and J. H. Wendell [9]. In inserting the formulations into the differential equations, products of the perturbationvalues of second and higher order occur which can be disregarded as opposed to the linear content. The result for the coriolis force for example is shown in the appendix. Therefore the cyclic variable components of the coriolis force are included as a result of the introduction of multiblade coordinates. On the other hand, in the case of a pure irregularity formulation one would only take the influence of the conus angle into consideration.

The basic values a_o, a_1, b_1, e_o, e_1 and f_1 are determined in a trimming calculation. As all 4 blades must possess the same conus angle of the flap motion which results from the equilibrium of the weight of the blade, lift and elastic restoring force, $b_o = 0$ can be immediately inserted. Accordingly a common angle of the lag motion results from the elastic restoring forces and air drag so that $f_o = C$. After inserting the trimm values calculated in the stationary state into the differential equation system the right sides of this become 0. Thus one obtains a linear homogenous differential equation system with periodic coefficients. The coordinates which describe the motion are thus

$$\Delta x, \ \Delta y, \ \Delta\phi, \ \Delta\Theta, \ \Delta a_o, \ \Delta a_1, \ \Delta b_1, \ \Delta b_o, \ \Delta e_o, \ \Delta e_1, \ \Delta f_1, \ \Delta f_o .$$

5. Methods of Solution

The equations of motion can be summarized in a differential equation system of second order

$$\underline{M}(t) \ \ddot{\underline{x}} + \underline{D}(t) \ \dot{\underline{x}} + \underline{C}(t) \ \underline{x} = \underline{0} \quad .$$

With the help of a simple transformation these equations can be returned to a differential equation system of the first order:

$$\dot{\underline{y}} + \underline{A}(t) \ \underline{y} = \underline{0} \quad .$$

To calculate the transition matrix $\underline{\Phi}(t)$, respectively the Monodromy-matrix $\underline{\Phi}(T)$, the differential equation system is integrated numerically by way of a rotor rotation. The initial conditions are

$$\underline{y}_k^T(t=o) = [\ y_1 \quad y_2 \quad y_3 \cdots y_i \cdots\ ] \qquad \text{where} \quad y_i=0 \quad \text{for } i\neq k \qquad \text{and} \quad y_i=1 \quad \text{for } i=k \quad .$$

The eigenvalues Λ_k of the Monodromy matrix also named characteristic multipliers directly allow an assessment of the stability of the equations of motion:

- if all $|\Lambda_k|$ are less than 1, then asymptotic stability is present
- if there is at least one $|\Lambda_k| > 1$, then the system is unstable
- if no characteristic multiplier with $|\Lambda_k|>1$ exists but one multiplier Λ_k with $|\Lambda_k|=1$ appears singularly (or however multiple in the case of full rank drop) then the system is weakly stable. Multiple multipliers with $|\Lambda_k|=1$ without complete rank drop cause instability.

According to Liapunow's Law of Reducability there exists a system with constant coefficients for every differential equation system with periodic coefficients. The eigen values λ_k of this constant system matrix can be calculated from those of the Monodromy matrix as follows:

$$\lambda_k = \frac{1}{T} \ln \Lambda_k = \delta_k + i\omega_k^*$$

The real part δ_k is obtained thus from:

$$\delta_k = \frac{1}{T} \ln |\Lambda_k| \quad .$$

For the imaginary part ω_k^*

$$\omega_k^* = \frac{1}{T} \arg \Lambda_k$$

is valid. Because of the periodicity of the tan-function the actual frequencies ω_k can only be determined up to an unknown multiple of the rotor rotation frequency:

$$\omega_k = n\,\Omega \pm \frac{1}{T} \arg \Lambda_k \qquad (*)$$

To interpret these results resonance calculations for a three bladed helicopter were carried out using the Floquet theory and the classic theory according to R. P. Coleman and A. M. Feingold. In Fig. 4 the eigenvalues determined by both methods are compared. If the frequency ω^*determined by Floquet theory is plotted against the rotor frequency it is shown that all frequencies lie below the $\Omega/2$ axis. Therefore, in Feingold and Coleman's diagram multiples of $\Omega/2$ have been centered as straight lines through the point of origin. The comparison of the two diagrams shows that a break always arises on the $\Omega/2$ straight line in the Floquet diagram when the frequency curve according to Coleman/Feingold intersects a straight line with an odd multiple of $\Omega/2$. The break in the ω^*curve arises on the abscissa when the frequency curve according to Coleman/Feingold intersects a straight line with even multiples of $\Omega/2$. This connection also results directly from the equation (*). However the comparison of the diagrams shows moreover.

1. If the ω^*-curve touches the $\Omega/2$ axis or abscissa then the polarity of ω^* alternates.
2. If the ω^*-curve touches the $\Omega/2$ axis then the multiplicity in the rotor angular frequency is raised or lowered around 1, contrary to the polarity alternation of ω^*.

With the aid of these correlations the appropriate ω-curve is thus able to develope out of a ω^*curve. As a starting value to determine the multiplicity n the frequencies for the rotor rotation frequency $\Omega = 0$ are used and extrapolated on small rotation frequencies. If the frequencies ω in the range of small rotor rotation frequencies Ω do not likewise become very small as, for example, the airframe's resonant frequencies then the factor n must grow beyond all restraints. Moreover it has been shown that the width of the intersection of the Runge Kutta 4 step method of numerical integration must be intensely increased for smaller rotor rotation frequencies so that no facultatively good approximation of the frequencies could be reached for $\Omega = 0$.

For rotors with polar symmetry coordinates of the system with constant coefficients, the multiblade coordinates are explicitly given so that conclusions from the determined frequencies ω can be drawn to the dynamic properties of the system. However if the rotor blades possess different dynamic characteristics it is then not easy to find the coordinates of the relevant system with constant coefficients. In this case the temporal solution can be directly determined with the aid of the Floquet theory.
It results in:

$$\underline{y}(t) = \underline{\underline{B}}(t) \left(c_k\, e^{\lambda_k t} \right)$$

where $\underline{\underline{B}}(t)$ contains the eigenfunction $\underline{b}_k(t)$ as columns. As the resulting motion for the k-th eigenvalue arises also from the equation (as described in [9])

$$\underline{y}_k(t) = \underline{\underline{\Phi}}(t)\, \underline{b}_k(0)$$

the eigenfunction belonging to the k-th eigenvalue can be determined by

$$\underline{b}_k(t) = \underline{\Phi}(t)\ \underline{b}_k(0)\ e^{-\lambda_k t}$$

$\underline{\Phi}$ (t) is the transition matrix for all instants of time t already determined and stored in the stability analysis. $\underline{b}_k$ (o) is the characteristic vector of the Monodromy matrix belonging to the k-th eigenvalue. If the eigenvalues appear conjugate complex then the eigenfunctions $\underline{b}_k(t)$ are also conjugate complex. These conjugate complex pairs of eigenfunctions can however be summarized as described by C. E. Hammond [10] . From the eigenfunctions which can thus be numerically determined and plotted amplitudes and phases of individual degrees of freedom can thus be determined for every eigenvalue.

6. Results

First calculations were carried out for a helicopter with data as shown in Table 1. The airframe data describe a light helicopter with a stiff landing gear so that high natural frequencies arise in the airframe. Therefore if the uncoupled modes of the airframe are regarded, only one instability range is possible in a revolution range $\Omega < 60$ due to the lag-airframe coupling. In the process the critical revolution results to $\Omega = 52$ for the pitch motion of the airframe. The next highest critical revolution belonging to the airframe's roll motion is of the order $\Omega = 70\ \frac{1}{sec}$ and therefore outside the revolution range considered. The rotor data represent a hingeless, soft-in-plane rotor.

In the diagrams (Fig. 5a) and (Fig. 5b) the real parts of the eigenvalues, converted into the system with constant coefficients, are plotted over the rotor angular velocity. The results represented in Fig. 5a take the aerodynamic damping into consideration. The results of a calculation without aerodynamic damping are given in Fig. 5b. Therefore, as shown in the work of R. A. Ormiston [12]the density of air was taken to be zero. While in the calculation with aerodynamic damping all eigenvalues have a negative real part in which the half-life period can however be high, a considerable instability is to be recognised in the case without aerodynamic damping. The appertaining time, in which the amplitude increases to its double value, amounts to 1,1 sec. The aerodynamic damping therefore makes a considerable contribution to the helicopters stability.

If one considers the individual eigenvalues then it is shown that two eigenvalues appear doubled at each time. As described in the work of I. Dugundij and T. H. Wendell [9] the introduction of multi blade coordinates leads to a decoupling of the differential equation system in which summation mode a_o and difference mode b_o are described by way of the same differential equation. As all blades have the same dynamic properties in this example then an analogy of summation and difference mode must also arise in the calculation according to the Floquet theory. Therefore one of the two same eigenvalues will probably belong to a form of motion which includes the summation mode while the other describes the motion which includes the difference mode. As the addition and difference mode are introduced for the lagging as well as the flapping motion, two pairs of equal eigenvalues could therefore exist. A clear clarification can result by means of calculating the temporal solutions belonging to the doubled eigenvalues.

In the calculation with aerodynamic damping 4 eigenvalues, where two of them are equal, possess a (negative) real part which increases considerably with the rotor revolution. The values rise from $\approx -3{,}8$ at $\Omega = 8$ 1/sec to ≈ -20 at $\Omega = 59$ so that these values could not completely be listed in Fig. 5a. The accompanying eigenfunctions belong essentially to the flapping motion as the aerodynamic damping has its greatest influence there.

In Fig. 6 the imaginary parts ω^* belonging to curve 1 of the real parts are plotted as calculated by Floquet theory. In this case the frequency curve of the system with constant coefficients can be determined easily as the accompanying curve of the real parts shows a possible range of instability. In this range of instability ($\Omega = 52$ 1/sec) the frequency ω of the system with constant coefficients belonging to the curve 1 of real parts is well known:

it results in: $$\omega_{crit} = |\Omega_{crit} - \omega_\zeta|$$

and is equal to one of the natural frequency of the airframe. Using Floquet theory you can obtain:

$$|\Omega_{crit} - \omega_\zeta| = n\,\Omega_{crit} \pm \omega^* \quad ,$$

where ω^* is known from the calculation of the eigenvalues. In the range $\Omega > 12$ there exists only one possible solution: $n = o$. With this result it is possible to calculate the accompanying frequencies of the system with constant coefficients as a function of the rotor angular velocity. The result is shown in Fig. 6 as dotted line. The dashed lines belong to the imaginary part of the other eigenvalues of the system with constant coefficients.

If it is sure, that the introduction of multiblade coordinates transform the system with periodically varying parameters into a system with constant coefficients as in the case of same dynamic behavior of all rotor blades, all frequencies of this system can be determined by Floquet theory without executing the extensive transformation analytically. Since the eigenvectors of the system with constant coefficients are equal to the eigenvectors of the Monodromy matrix, the accompanying mode is well known. In this case the eigenfunction of the system with periodically varying parameters don't have to be calculated extensively.

However, due to reasons of time it was no longer possible to calculate and plot the characteristic functions and the eigenvectors of the Monodromy matrix to compare the temporal solutions in this paper. The influence of blade control as well as different mass, damping and stiffness distribution of the individual rotor blades could also not be considered. This is reserved for subsequent investigations.

Acknowledgement

The paper is based on research work funded by the Bundesministerium für Forschnung und Technologie BMFT (Ministry of Research and Technology), contract LFF 84318

References

[1] Coleman, R.P. Feingold, A.M. — Theory of Self-Excited Mechanical Oscillations of Helicopter Rotors with Hinged Blades, NACA Report 1351, 1958

[2] Schröder, R. — A Theory for Ground-Resonance of Helicopters covering Freedoms of Fuselage Rotation, Deutsche Forschungs- und Versuchsanstalt für Luft- und Raumfahrttechnik, Fachbericht DLR-FB 73-84, 1973

[3] Nahas, M.N. — Helicopter Ground Resonance - A Spatial Model Analysis, The Aeronautical Journal, Vol. 88, Number 877, 1984

[4] Schrage, D.P. Peters, D.A. — Effect of Structural Coupling Parameters on the Flap-Lag Forced Response of a Rotorblade in Forward Flight Using Floquet Theory, Fourth European Rotorcraft and Powered Lift Aircraft Forum, 1978, paper No. 23

[5] Just, W. — Aerodynamik der Hub- und Tragschrauber Teil 2, Berechnung des Rotors, Deutsche Studiengemeinschaft Hubschrauber e.V., 1954

[6] Reichert, G. — Flugeigenschaften bei Hubschraubern mit elastisch angeschlossenen Rotorblättern, Wissenschaftliche Gesellschaft für Flug- und Raumfahrttechnik, Jahrbuch 1963

[7] Johnson, W. — Helicopter Theory, Princeton, University Press, 1980

[8] Hohenemser, K.H. Yin, S.K. — Some Applications of the Method of Multiblade Coordinates, Journal of the American Helicopter Society, Vol. 17, No. 3, July 1972, pp. 3-12

[9] Dugundji, J. Wendell, J.H. — Some Analysis Methods for Rotating Systems with Periodic Coefficients, AIAA Journal, Vol. 21, No. 6, 1983

[10] Hammond, C.E. — An Application of Floquet Theory to Prediction of Mechanical Instability, Specialist Meeting on Rotorcraft Dynamics, AHS, 1974

[11] Peters, D.A. Hohenemser, K.H. Application of the Floquet Transition Matrix to Problems of Lifting Rotor Stability, Journal of the American Helicopter Society, Vol. 16 No. 2, April 1971, pp. 25-33

[12] Ormiston, R.A. Aeromechanical Stability of Soft Inplane Hingeless Rotor Helicopters Third European Rotorcraft and Powered Lift Aircraft Forum, paper No. 25, 1977

Appendix

Vektor from centre of gravity of the helicopter to one point of the blade:

$$\underline{r} = \begin{bmatrix} x_s \\ y_s \\ z_s \end{bmatrix} + a \begin{bmatrix} \cos\psi \\ \sin\psi \\ 0 \end{bmatrix} + e \begin{bmatrix} \cos\beta\cos\psi \\ \cos\beta\sin\psi \\ \sin\beta \end{bmatrix} + b \begin{bmatrix} \sin\zeta\sin\psi + \cos\zeta\cos\beta\cos\psi \\ -\sin\zeta\cos\psi + \cos\zeta\cos\beta\sin\psi \\ \cos\zeta\sin\beta \end{bmatrix} \tag{1}$$

Acceleration of one point of the blade:

$$\begin{aligned} \ddot{\underline{r}} = {} & \Omega^2 \begin{bmatrix} -(a + e\cos\beta + b\cos\zeta\cos\beta)\cos\psi - b\sin\zeta\sin\psi \\ -(a + e\cos\beta + b\cos\zeta\cos\beta)\sin\psi + b\sin\zeta\cos\psi \\ 0 \end{bmatrix} \\ & + \dot{\Omega} \begin{bmatrix} -(a + e\cos\beta + b\cos\zeta\cos\beta)\sin\psi + b\sin\zeta\cos\psi \\ (a + e\cos\beta + b\cos\zeta\cos\beta)\cos\psi + b\sin\zeta\sin\psi \\ 0 \end{bmatrix} \\ & + 2\,\Omega\dot{\beta} \begin{bmatrix} -(-e\sin\beta - b\cos\zeta\sin\beta)\sin\psi \\ (-e\sin\beta - b\cos\zeta\sin\beta)\cos\psi \\ 0 \end{bmatrix} + 2\,\Omega\dot{\zeta} \begin{bmatrix} -(-b\sin\zeta\cos\beta)\sin\psi + b\cos\zeta\cos\psi \\ (-b\sin\zeta\cos\beta)\cos\psi + b\cos\zeta\sin\psi \\ 0 \end{bmatrix} \\ & + \dot{\zeta}^2 \begin{bmatrix} (-b\cos\zeta\cos\beta)\cos\psi - b\sin\zeta\sin\psi \\ (-b\cos\zeta\cos\beta)\sin\psi + b\sin\zeta\cos\psi \\ (-b\cos\zeta)\sin\beta \end{bmatrix} + \ddot{\zeta} \begin{bmatrix} (-b\sin\zeta\cos\beta)\cos\psi + b\cos\zeta\sin\psi \\ (-b\sin\zeta\cos\beta)\sin\psi - b\cos\zeta\cos\psi \\ (-b\sin\zeta)\sin\beta \end{bmatrix} \\ & + 2\dot{\zeta}\dot{\beta} \begin{bmatrix} (b\sin\zeta\sin\beta)\cos\psi \\ (b\sin\zeta\sin\beta)\sin\psi \\ (-b\sin\zeta\cos\beta) \end{bmatrix} + \dot{\beta}^2 \begin{bmatrix} -(+e\cos\beta + b\cos\zeta\cos\beta)\cos\psi \\ -(+e\cos\beta + b\cos\zeta\cos\beta)\sin\psi \\ -(e + b\cos\zeta)\sin\beta \end{bmatrix} \\ & + \ddot{\beta} \begin{bmatrix} -(+e\sin\beta + b\cos\zeta\sin\beta)\cos\psi \\ -(+e\sin\beta + b\cos\zeta\sin\beta)\sin\psi \\ (e + b\cos\zeta)\cos\beta \end{bmatrix} + \begin{bmatrix} \ddot{x} \\ \ddot{y} \\ 0 \end{bmatrix} \\ & + \begin{bmatrix} \ddot{\Theta}[(e + b\cos\zeta)\sin\beta + z_s] \\ -\ddot{\Phi}[(e + b\cos\zeta)\sin\beta + z_s] \\ \ddot{\Phi}[(a + e\cos\beta + b\cos\zeta\cos\beta)\sin\psi - b\sin\zeta\cos\psi + y_s] - \ddot{\Theta}[(a + e\cos\beta + b\cos\zeta\cos\beta)\cos\psi \\ \qquad + b\sin\zeta\sin\psi + x_s] \end{bmatrix} \end{aligned} \tag{2}$$

$$+\begin{bmatrix} \dot\theta\dot\phi[(a + e\cos\beta + b\cos\zeta\cos\beta)\sin\psi - b\sin\zeta\cos\psi + y_s] - \dot\theta^2[(a + e\cos\beta + b\cos\zeta\cos\beta)\cos\psi \\ \qquad + b\sin\zeta\sin\psi + x_s] \\ -\dot\phi^2[(a + e\cos\beta + b\cos\zeta\cos\beta)\sin\psi - b\sin\zeta\cos\psi + y_s] - \dot\theta\dot\phi[(a + e\cos\beta + b\cos\zeta\cos\beta)\cos\psi \\ \qquad + b\sin\zeta\sin\psi + x_s] \\ -\dot\phi^2[(e + b\cos\zeta)\sin\beta + z_s] - \dot\theta^2[(e + b\cos\zeta)\sin\beta + z_s] \end{bmatrix}$$

$$+\begin{bmatrix} 0 \\ 0 \\ 2\dot\Omega[(a + e\cos\beta + b\cos\zeta\cos\beta)\cos\psi + b\sin\zeta\sin\psi] - 2\dot\Omega[-(a + e\cos\beta + b\cos\zeta\cos\beta)\sin\psi \\ \qquad + b\sin\zeta\cos\psi] \end{bmatrix}$$

$$+\begin{bmatrix} +2\dot\theta\dot\zeta(-b\sin\zeta)\sin\beta \\ -2\dot\phi\dot\zeta(-b\sin\zeta)\sin\beta \\ +2\dot\phi\dot\zeta[(-b\sin\zeta\cos\beta)\sin\psi - b\cos\zeta\cos\psi] - 2\dot\theta\dot\zeta[(-b\sin\zeta\cos\beta)\cos\psi + b\cos\zeta\sin\psi] \end{bmatrix}$$

$$+\begin{bmatrix} +2\dot\theta\dot\beta(e + b\cos\zeta)\cos\beta \\ -2\dot\phi\dot\beta(e + b\cos\zeta)\cos\beta \\ +2\dot\phi\dot\beta[(e\sin\beta - b\cos\zeta\sin\beta)\sin\psi] - 2\dot\theta\dot\beta[(-e\sin\beta - b\cos\zeta\sin\beta)\cos\psi] \end{bmatrix}$$

Velocity normal to the blade:

$$V_n = \dot x\,\beta\cos\psi + \dot y\,\beta\sin\psi + \dot\theta[(a + e + b + z_s\,\beta)\cos\psi + x_s] - \dot\phi[(a + e + b + z_s\,\beta)\sin\psi + y_s] + \dot\zeta\, b\,\zeta\,\beta - \dot\beta[e + b] - w_i \tag{3}$$

Velocity tangential to the blade:

$$V_t = -\dot x\sin\psi + \dot y\cos\psi - \dot\theta[(e + b)\beta + z_s]\sin\psi - \dot\phi[(e + b)\beta + z_s]\cos\psi + \Omega(a + e + b) - \dot\zeta\, b \tag{4}$$

Coriolis force: (5)

$$\begin{aligned} dF_{co} = {} & dm\,2\,\Omega\,(e + b)\,[\Delta a_o(a_1\,\Omega\sin\psi_k - b_1\,\Omega\cos\psi_k) + \Delta a_1(a_o\,\Omega\sin\psi_k - 2a_1\,\Omega\cos\psi_k\sin\psi_k - b_1\Omega) \\ & + \Delta b_1(-a_o\,\Omega\cos\psi_k - a_1\Omega + 2b_1\,\Omega\sin\psi_k\cos\psi_k) + \Delta\dot a_o(-a_1\cos\psi_k - b_1\sin\psi_k) \\ & + \Delta\dot a_1(-a_o\cos\psi_k + a_1\cos^2\psi_k + b_1\cos\psi_k\sin\psi_k) + \Delta\dot b_1(-a_o\sin\psi_k + a_1\cos\psi_k\sin\psi_k + b_1\sin^2\psi_k) \\ & + \Delta b_o(a_1\,\Omega\sin\psi_k(-1)^{k-1} - b_1\,\Omega\cos\psi_k(-1)^{k-1}) + \Delta\dot b_o(a_o(-1)^{k-1} - a_1\cos\psi_k(-1)^{k-1} - b_1\sin\psi_k(-1)^{k-1}) \\ & + a_o\,a_1\,\Omega\sin\psi_k - a_o\,b_1\,\Omega\cos\psi_k - a_1^2\,\Omega\cos\psi_k\sin\psi_k - a_1\,b_1\,\Omega \quad + \text{ nonlinear terms }] \end{aligned}$$

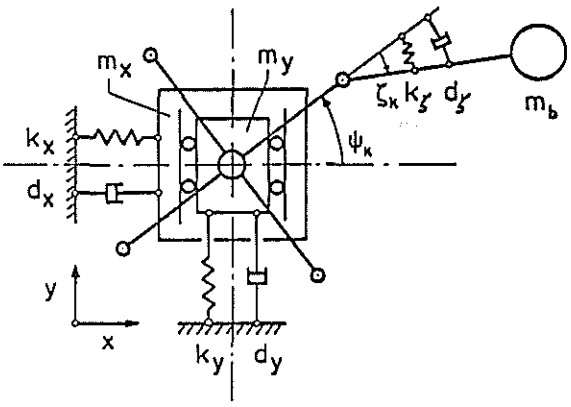

Figure 1. Planar model for ground resonance investigations

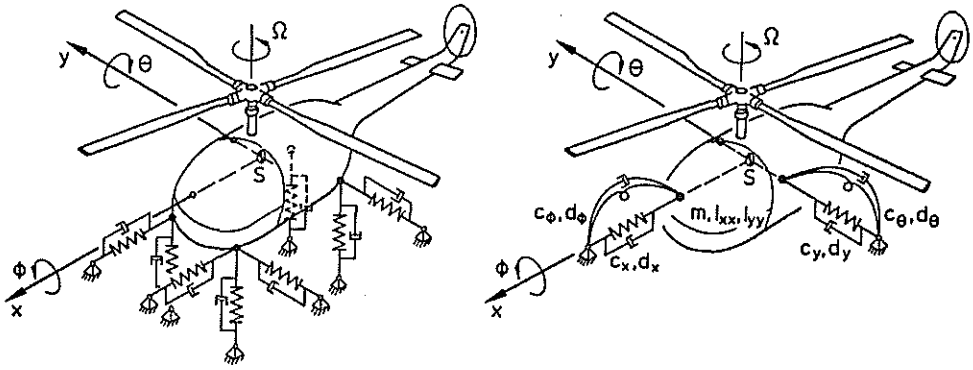

Figure 2. Spatial model of fuselage with landing gear

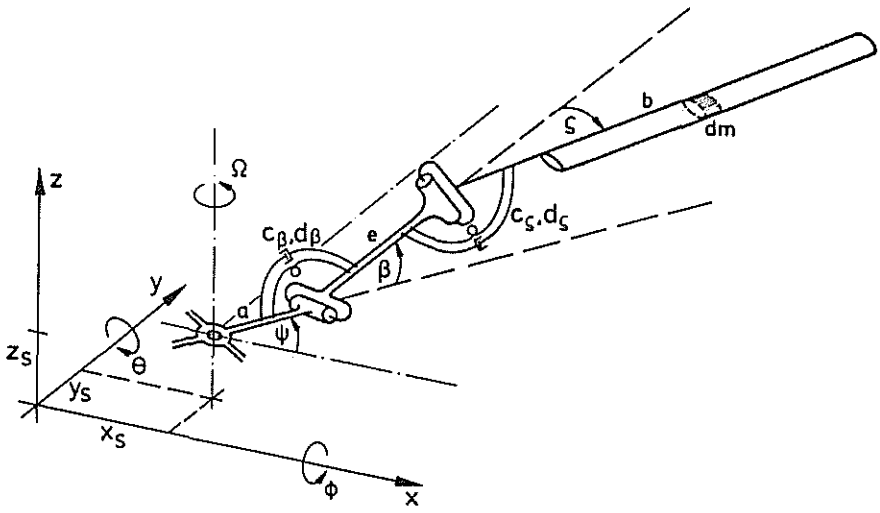

Figure 3. Mechanical system representing one rotor blade

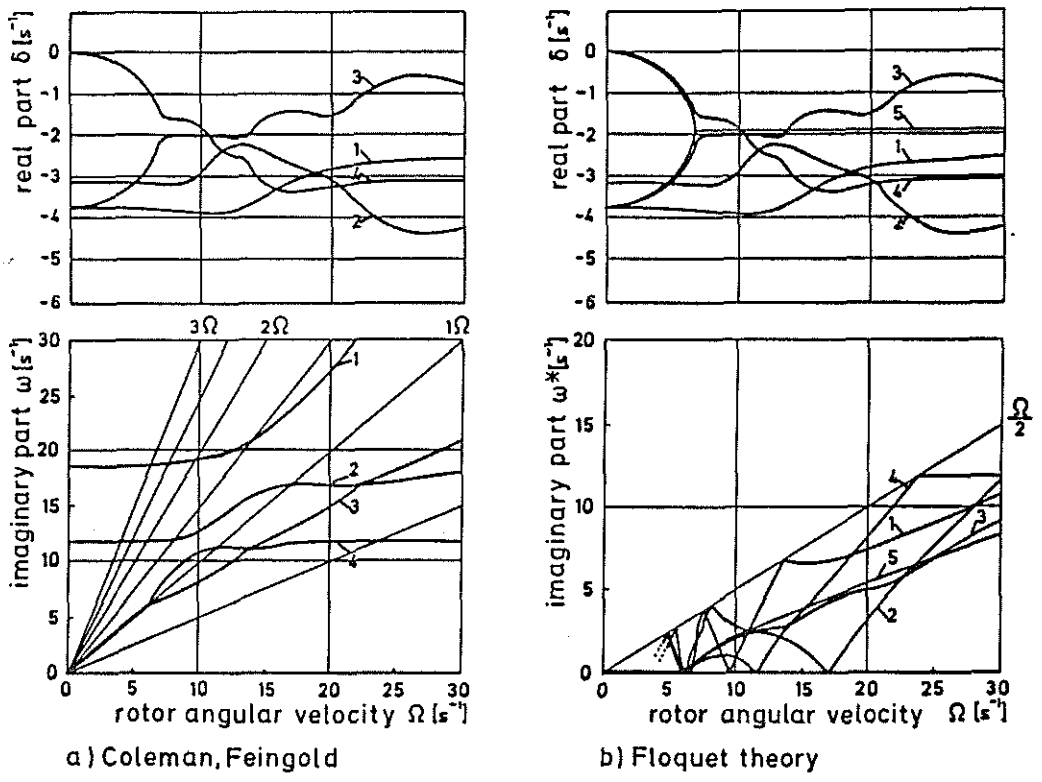

Figure 4. Real and imaginary part of eigenvalues

Data of fuselage:		
Mass (m)	-	2400 kg
Moment of inertia in roll (I_{xx})	-	1500 kg m²
Moment of inertia in pitch (I_{yy})	-	4500 kg m²
Longitudinal damping (d_x)	-	1500 kg/s
Latitudinal damping (d_y)	-	1500 kg/s
Damping in roll (d_ϕ)	-	16000 kg m²/s
Damping in pitch (d_θ)	-	15000 kg m²/s
Longitudinal stiffness (c_x)	-	3840000 kg/s²
Latitudinal stiffness (c_y)	-	3840000 kg/s²
Stiffness in roll (c_ϕ)	-	1422000 kg m²/s²
Stiffness in pitch (c_θ)	-	1422000 kg m²/s²
Data of blades:		
Number of blades	-	4
Rotor radius (R)	-	5 m
Radial position of lag hinge (a)	-	0,75 m
Distance lag hinge to drag hinge (e)	-	0,07 m
Mass of blade (m_b)	-	24 kg
Blade moment of inertia about drag hinge	-	134 kg m²
Blade moment of inertia about lag hinge	-	130 kg m²
Flap damper (d_β)	-	250 kg m²/s
Lag damper (d_ζ)	-	420 kg m²/s
Flap spring (c_β)	-	8000 kg m²/s²
Lag spring (c_ζ)	-	37500 kg m²/s²

Table 1. Data

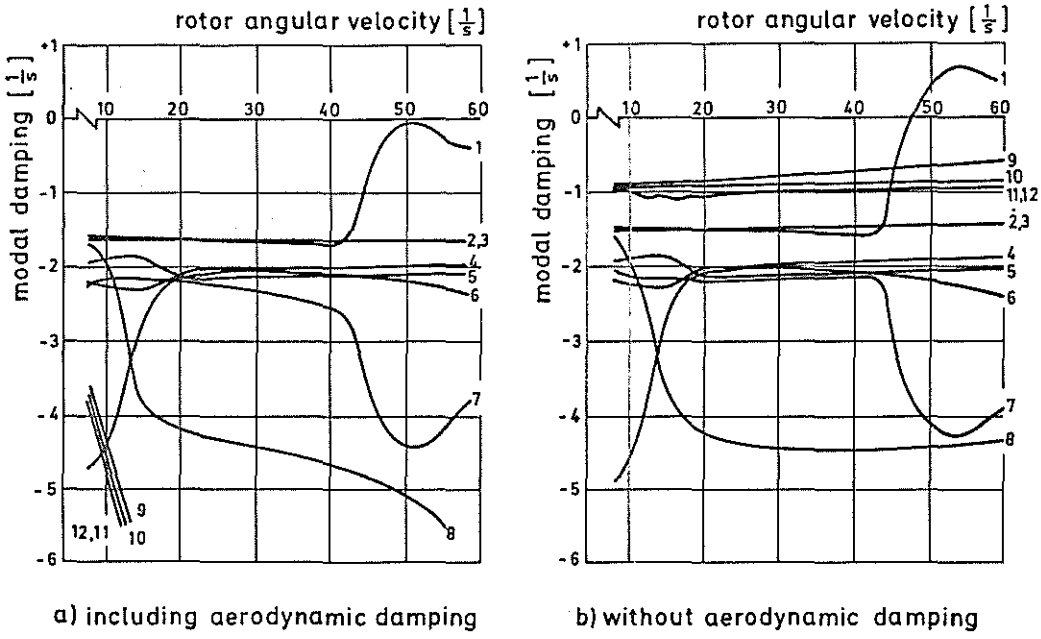

Figure 5. Real part of eigenvalues of corresponding system with constant parameters

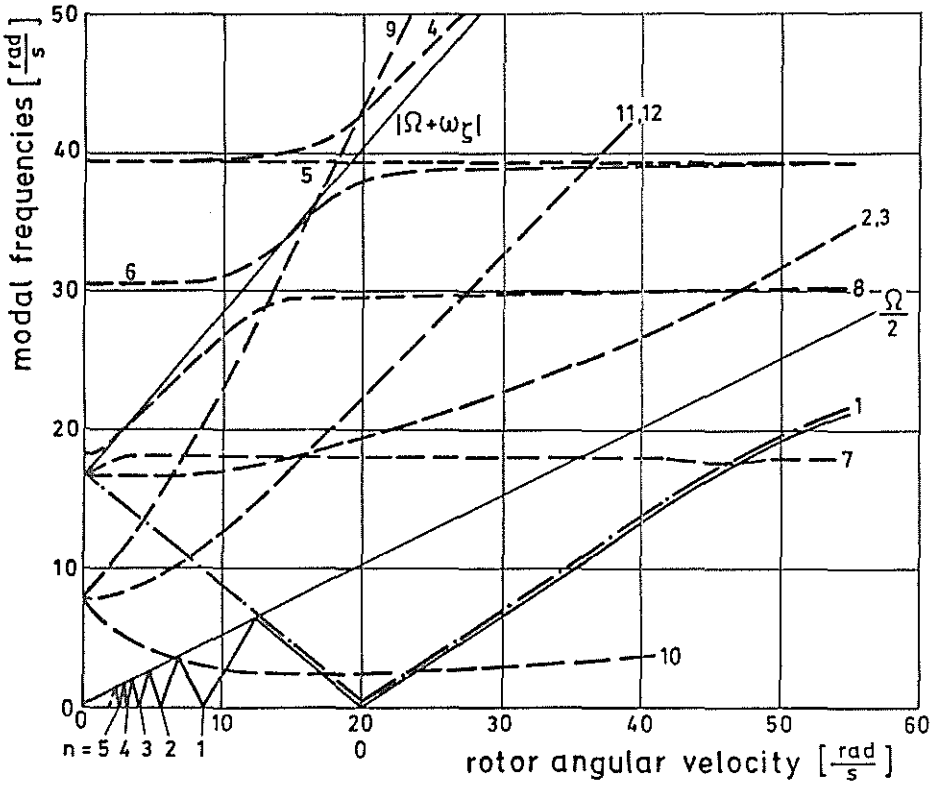

Figure 6. Imaginary part of eigenvalues of corresponding system with constant parameters (including aerodynamic damping)